The LMTO object of the CP-PAW code

Peter E. Blöchl

Institute of Theoretical Physics; Clausthal University of Technology;
D-38678 Clausthal Zellerfeld; Germany;
http://www.pt.tu-clausthal.de/atp/

Contents

Chapter 1

Todo

1.1 Fixes

- lmto_overlapphi calculates the onsite overlap matrix of partial waves in a sphere.
- using only sp like tight-binding orbitals and local exchange lead to an increase of the band gap of silicon above 1.3 eV. After adding the d-orbitals to the HF term collapsed the band gap dramatically below the dft value. Core-valence echange seems to have an important effect on the band gap too.
- double counting in `paw_lmto` and `paw_dmft` is in error. It takes the partial wave density matrix do do it properly. currently only the density of AEF is used.
- The charge sumrule is not correct! The calculation for an H-atom yields $Tr[\rho O] \approx 0.2$. The problem is not the difference between tailed orbitals and the multicenter expansion, because $(r * \chi)^2$ agrees quire well.

1.2 Ideas

- With the introduction of the tailed representation of the NTBO's we **switch from a multi-center expansion to a one-center expansion**. This, however, requires to increase the number of angular momenta for the tail functions beyond that used for the augmentation: Each (screening) Hankel function centered on the neighboring site contributes arbitrary many angular momenta at the central site.

  The tail functions for the higher angular momenta behave, at the central site, like a bare Bessel function. Beyond the central site, we can add the same pairs of exponential tails as for the lower tailed partial waves.

  (The following is probably no more true. please check!) Currently we use the following rule: Rule: (1) Each head function has exactly one tail function attributed to it. Thus we can identify the phidot function uniquely by looking for the tail function with the correct angular momentum. From (1) follows, that there is at most one tail function per site and angular momentum.

- Suggestion: the exponential functions for the tailed expansion are determined by trial and error. A more systematic approach for the tail function would be to (1) build a Hankel function on a neighboring site, which is augmented by (a) a bare Bessel function and (b) by a screened scattering partial wave $|\dot{\bar{p}}hi\rangle$. (1a) In order to make the formulation less dependent on the neighbor distance, we could also include the gradients of these functions. (2) These functions are expanded about the central site into an angular-momentum expansion. (3) a reasonably weighted least-square fit of the exponential tails to these functions will provide a "optimum shape" of the tails for each angular momentum.

- The orbitals in the tailed one-center expansion and as multicenter expansions can be compared using `LMTO_PLOTORBS`. Calculations for hydrogen suggest that a good choice is $K2 = -1.$ and $(\lambda_1, \lambda_2) = (4, 2)$. The rationale for $K2$ is that the energy of the hydrogen orbital is at $-1Ry = -\frac{1}{2}H = \frac{1}{2}K2$. (see `Dummy/Sitest/Test/Occtest/H2test`)

Chapter 2

Purpose and theoretical background of the LMTO Object

The LMTO object maps the wave functions expressed in augmented plane waves onto a basiset of **natural tight-binding orbitals**. The natural tight-binding orbitals are a kind of LMTO's, screened such that the tails exhibit only scattering character in the context of nodeless wave functions[1].

2.1 Augmentation

The concept of linear augmented waves[2] is as follows:

1. At first, a so-called **envelope function** $|K_\alpha^\infty\rangle$ is defined.[1]

2. In a second step, this envelope function is expanded about each atomic site into spherical harmonics. More generally, they are expanded into **head functions** $|K_\alpha^\Omega\rangle$ and **tail functions** $|J_\alpha^\Omega\rangle$. The head function is the dominant contribution and carries the quantum number of the final orbital, while the tail functions are the minor contributions with different quantum numbers. In practice, the head functions are solid Hankel functions and the tail functions are solid Bessel functions.

$$|K_\alpha^\infty\rangle = |K_\alpha^\Omega\rangle - \sum_\beta |J_\beta^\Omega\rangle S_{\beta,\alpha}^\dagger + |K_\alpha^I\rangle \tag{2.1}$$

   The coefficients $S_{\alpha,\beta}$ of the tail functions are called **structure constants**.

   The difference between the full envelope function and its expansion into head and tail functions is the **interstitial envelope function**[2] $|K_\alpha^I\rangle$.

[1] The superscript ∞ denotes that the function extends over all space, a superscript Ω denotes that the function is truncated (set to zero) outside the augmentation sphere Ω_R centerd at the site denoted by the index. The superscript I denotes that the function is limited to the interstitial region, that is outside all augmentation spheres. If the augmentation spheres overlap, the function in the interstitial region is defined by subtraction of all sphere contributions.

[2] The interstitial envelope function is confined mostly in the region in between the atoms, but it also accounts for the overlap of the atomic regions and so-called higher partial waves not taken care of in the regular partial-wave expansion.

3. In the third step the head and tail functions are replaced differentially at some sphere radius by **partial waves** of the atomic potential. For that purpose, we use as partial waves a solution of the Schrödinger equation for some energy, denoted as $|\phi_\alpha\rangle$ and its energy derivative function $|\dot{\phi}_\alpha\rangle$.

   The matching parameters are called **potential parameters**.

2.2 Structure constants

2.2.1 Hankel functions as envelope function

In practice, we will use solid Hankel functions $H_L(\vec{r})$ as envelope functions, so that

$$\langle \vec{r}|K^{\infty}_{R,L}\rangle = H_L(\vec{r}-\vec{R}) \tag{2.2}$$

Solid Hankel functions are irregular solutions of the the inhomogeneous Helmholtz equation[3]

$$\left[\vec{\nabla}^2 + k^2\right] H_L(\vec{r}) = -4\pi(-1)^\ell \mathcal{Y}(\vec{\nabla})\delta(\vec{r}) \tag{2.3}$$

Here $\mathcal{Y}_\ell(\vec{r}) = r^\ell Y_\ell(\vec{r})$ is a polynomial. With a gradient as argument, it becomes a differential operator.

Further detail about the Hankel and Bessel functions can be found in appendix A.

2.2.2 Hankel and Bessel functions as head and tail functions

Defining the envelope function via an isotropic and translationally invariant differential equation of second order has the advantage that the solution can be expanded about different centers into regular solutions of the same differential equation with specific angular momenta. The regular solutions of the Helmholtz equation are the Bessel functions.

Hankel and Bessel functions are defined[4] so that they behave at the origin as

$$K^{\Omega}_{R,L}(\vec{r}) = \left[(2\ell-1)!!\frac{1}{|\vec{r}-\vec{R}|^{\ell+1}} + \ldots\right] Y_L(\vec{r}-\vec{R})\theta_{\Omega_R}(\vec{r}) \tag{2.4}$$

$$J^{\Omega}_{R,L}(\vec{r}) = \left[\frac{1}{(2\ell+1)!!}|\vec{r}-\vec{R}|^{\ell+1} + \ldots\right] Y_L(\vec{r}-\vec{R})\theta_{\Omega_R}(\vec{r}) \tag{2.5}$$

$\theta_{\Omega_R}(\vec{r})$ is a step function, that is, one within the augmentation region Ω_R centered at site R, while it vanishes outside. The terms neglected are higher orders in $|\vec{r}-\vec{R}|$.

2.2.3 Bare structure constants

The **bare structure constants** $S^{\dagger}_{\beta,\alpha}$ are the expansion constants for an off-center expansion of solid spherical Hankel functions $|K^{\infty}_{\alpha}\rangle$ into **solid Bessel functions** $|J^{\Omega}_{\beta}\rangle$.

$$|K^{\infty}_{\alpha}\rangle = |K^{\Omega}_{\alpha}\rangle - \sum_{\beta} |J^{\Omega}_{\beta}\rangle S^{\dagger}_{\beta,\alpha} + |K^{I}_{\alpha}\rangle \tag{2.6}$$

[3] I am not sure whether also the three dimensional differential equation or only the one-dimensional differential equation for the radial part is called Helmholtz equation.

[4] This is our definition, not a generally accepted convention.

The index α denotes here an atomic site R and a set of angular momenta $L = (\ell, m)$.

The superscript ∞ denotes that the function extends over all space, a superscript Ω denotes that the function is truncated (set to zero) outside the augmentation sphere Ω_R centered at the site denoted by the index. The superscript I denotes that the function is limited to the interstitial region, that is, outside all augmentation spheres. If the augmentation spheres overlap, the function in the interstitial region is defined by subtraction of all sphere contributions.

BARE STRUCTURE CONSTANTS

The bare structure constants have the form

$$S_{RL,R'L'} = (-1)^{\ell'+1} 4\pi \sum_{L''} C_{L,L',L''} H_{L''}(\vec{R}' - \vec{R}) \begin{cases} (-ik)^{\ell+\ell'-\ell''} & \text{for } k^2 > 0 \\ \delta_{\ell+\ell'-\ell''} & \text{for } k^2 = 0 \\ \kappa^{\ell+\ell'-\ell''} & \text{for } k^2 = -\kappa^2 < 0 \end{cases} \tag{2.7}$$

With $C_{L,L',L''}$, we denote the **Gaunt coefficients** defined by

$$Y'_L(\vec{r}) Y_{L''}(\vec{r}) = \sum_L Y_L(\vec{r}) C_{L,L',L''} \tag{2.8}$$

Note, that the Gaunt coefficients for spherical and real spherical harmonics differ.[5]

The bare structure constants are hermitean[6], i.e.

$$S_{RL,R'L'} = S_{R'L',RL} \tag{2.9}$$

This is, however, not true for each angular-momentum block individually, i.e. in general we have $S_{RL,R'L'} \neq S_{R,L',R'L}$.

2.2.4 Screened structure constants

A so-called **screened LMTO representations** is defined by a set of screened scattering partial waves $|\dot{\bar{\phi}}_\alpha\rangle$. In what we call the nodeless-representation, the scattering partial waves are defined as nodeless scattering wave functions.

The node-less scattering partial wave $|\dot{\bar{\phi}}_\alpha\rangle$ define the screening constants $\bar{Q}_\alpha$ such that the screened tail functions $|\bar{J}_\alpha\rangle$ match with value and derivative to the scattering partial wave

$$|\dot{\bar{\phi}}_\alpha\rangle \rightarrow |\bar{J}^\Omega_\alpha\rangle \stackrel{\text{def}}{=} |J^\Omega_\alpha\rangle - |K^\Omega_\alpha\rangle \bar{Q}_\alpha \tag{2.10}$$

A screened solid Hankel function $|\bar{K}^\infty_\alpha\rangle$ is a superposition of bare solid Hankel functions on a set of atomic positions

$$|\bar{K}^\infty_\alpha\rangle = \sum_\beta |K^\infty_\beta\rangle c_{\beta,\alpha} \tag{2.11}$$

[5] In practice, we use real spherical harmonics and the corresponding Gaunt coefficients.

[6] We use that $H_L(\vec{r}) = (-1)^\ell H_L(-\vec{r})$ and that the Gaunt coefficients $C_{L,L',L''}$ vanish unless $\ell + \ell' + ''$ is even.

with the property that the tail functions are made entirely from screened Bessel functions $|\bar{J}^{\Omega}_{\beta}\rangle$, i.e.

$$|\bar{K}^{\infty}_{\alpha}\rangle = |K^{\Omega}_{\alpha}\rangle - \sum_{\beta} |\bar{J}^{\Omega}_{\beta}\rangle \bar{S}^{\dagger}_{\beta,\alpha} + |\bar{K}^{I}_{\alpha}\rangle \tag{2.12}$$

The expansion coefficients $\bar{S}$ are the screened structure constants.

By equating the two expressiones for the screened Hankel functions, namely Eq. 2.11 and Eq. 2.12, we can extract the screened structure constants and the superposition coeffcients.

$$\sum_{\beta}\Big[|K^{\Omega}_{\beta}\rangle - \sum_{\gamma}|J^{\Omega}_{\gamma}\rangle S^{\dagger}_{\gamma,\beta} + |K^{I}_{\beta}\rangle\Big] c_{\beta,\alpha} = |K^{\Omega}_{\alpha}\rangle - \sum_{\beta}\underbrace{\Big[|J^{\Omega}_{\beta}\rangle - |K^{\Omega}_{\beta}\rangle\bar{Q}_{\beta}\Big]}_{|\bar{J}^{\Omega}_{\beta}\rangle}\bar{S}^{\dagger}_{\beta,\alpha} + |\bar{K}^{I}_{\alpha}\rangle$$

$$\sum_{\beta}|K^{\Omega}_{\beta}\rangle c_{\beta,\alpha} - \sum_{\beta,\gamma}|J^{\Omega}_{\gamma}\rangle S^{\dagger}_{\gamma,\beta} c_{\beta,\alpha} = \sum_{\beta}|K^{\Omega}_{\beta}\rangle\Big[\delta_{\beta,\alpha} + \bar{Q}_{\beta}\bar{S}^{\dagger}_{\beta,\alpha}\Big] - \sum_{\beta}|J^{\Omega}_{\beta}\rangle\bar{S}^{\dagger}_{\beta,\alpha} \tag{2.13}$$

By comparing the coefficients, we obtain

$$c_{\beta,\alpha} = \delta_{\beta,\alpha} + \bar{Q}_{\beta}\bar{S}^{\dagger}_{\beta,\alpha} \tag{2.14}$$

$$\bar{S}^{\dagger}_{\gamma,\alpha} = \sum_{\beta} S^{\dagger}_{\gamma,\beta} c_{\beta,\alpha} \tag{2.15}$$

which can be resolved to [7] the defining equation of the screened structure constants

SCREENED STRUCTURE CONSTANTS

$$\bar{\boldsymbol{S}}^{\dagger} = \boldsymbol{S}^{\dagger}\Big[\mathbf{1} - \boldsymbol{S}^{\dagger}\bar{\boldsymbol{Q}}\Big]^{-1} \tag{2.17}$$

and the expression of the screened Hankel functions

$$|\bar{K}^{\infty}_{\alpha}\rangle = \sum_{\beta}|K^{\infty}_{\beta}\rangle\Big[\delta_{\beta,\alpha} + \bar{Q}_{\beta}\bar{S}^{\dagger}_{\beta,\alpha}\Big]\,. \tag{2.18}$$

Because, we calculate the screened structure constants on finite clusters, Eq. 2.17 should be considered of only formal value and should not be used in the actual calculations. Rather, the defining equations Eq. 2.15 shall be used as shown in the following section.

2.3 Screening on finite clusters

The screened structure constants are calculated on a cluster of atomic sites. The calculation can, in principle, be done for each single screened Hankel function independently. In practice, we do the calculations for all atoms centered on a given site in one step.

[7]

$$\begin{aligned} \boldsymbol{c} = \mathbf{1} + \bar{\boldsymbol{Q}}\bar{\boldsymbol{S}}^{\dagger} = \mathbf{1} + \bar{\boldsymbol{Q}}\boldsymbol{S}^{\dagger}\boldsymbol{c} \quad &\Rightarrow \quad \sum_{\gamma}\Big[\delta_{\beta,\gamma} - \bar{Q}_{\beta}S^{\dagger}_{\beta,\gamma}\Big]c_{\gamma,\alpha} = \delta_{\beta,\alpha} \quad \Rightarrow \quad \boldsymbol{c} = [\mathbf{1} - \bar{\boldsymbol{Q}}\boldsymbol{S}^{\dagger}]^{-1} \\ \bar{\boldsymbol{S}}^{\dagger} = \boldsymbol{S}^{\dagger}\boldsymbol{c} = \boldsymbol{S}^{\dagger}[\mathbf{1} - \bar{\boldsymbol{Q}}\boldsymbol{S}^{\dagger}]^{-1} \quad &\Leftrightarrow \quad [\mathbf{1} - \boldsymbol{S}\bar{\boldsymbol{Q}}]\bar{\boldsymbol{S}} = \boldsymbol{S} \end{aligned} \tag{2.16}$$

We go back to the defining equation system Eq. 2.14, Eq. 2.15 and rewrite it in terms of vectors, which are defined on the cluster B. The index α labeling the vectors correspond to the envelope functions centered at the central site.

The equations attain the form

$$\vec{c}_\alpha \overset{\text{Eq. } 2.14}{=} \vec{e}_\alpha + \bar{\boldsymbol{Q}}\vec{s}_\alpha \tag{2.19}$$

$$\vec{s}_\alpha \overset{\text{Eq. } 2.15}{=} \boldsymbol{S}^\dagger \vec{c}_\alpha \tag{2.20}$$

where the vectors $\vec{c}$, $\vec{s}_\alpha$ and $\vec{e}_\alpha$ are defined by its components

$$\begin{aligned}\left(\vec{c}_\alpha\right)_\beta &= c_{\beta,\alpha}\\ \left(\vec{s}_\alpha\right)_\beta &= \bar{S}^\dagger_{\beta,\alpha}\\ \left(\vec{e}_\alpha\right)_\beta &= \delta_{\beta,\alpha}\end{aligned} \tag{2.21}$$

$$\begin{aligned} & & \vec{c}_\alpha &\overset{\text{Eq. } 2.19}{=} \vec{e}_\alpha + \bar{\boldsymbol{Q}}\vec{s}_\alpha \overset{\text{Eq. } 2.20}{=} \vec{e}_\alpha + \bar{\boldsymbol{Q}}\boldsymbol{S}^\dagger\vec{c}_\alpha\\ \Rightarrow \quad & \left[\mathbf{1} - \bar{\boldsymbol{Q}}\boldsymbol{S}^\dagger\right]\vec{c}_\alpha &&= \vec{e}_\alpha\\ \Rightarrow \quad & \vec{c}_\alpha &&= [\mathbf{1} - \bar{\boldsymbol{Q}}\boldsymbol{S}^\dagger]^{-1}\vec{e}_\alpha\\ & \vec{s}_\alpha &&\overset{\text{Eq. } 2.20}{=} \boldsymbol{S}^\dagger\vec{c}_\alpha = \boldsymbol{S}^\dagger[\mathbf{1} - \bar{\boldsymbol{Q}}\boldsymbol{S}^\dagger]^{-1}\vec{e}_\alpha \end{aligned} \tag{2.22}$$

Interestingly the vector on the right-hand side $\vec{e}_\alpha$ can not be simply ignored as the matrix form suggests. This is specific to the calculation on the cluster. Because of this we cannot identify the contribution of these vectors with a unit matrix.

CALCULATION OF SCREENED STRUCTURE CONSTANTS

Thus, we first evaluate the bare structure constants $\boldsymbol{S}^\dagger$ on the cluster, and from that $[\mathbf{1} - \bar{\boldsymbol{Q}}\boldsymbol{S}^\dagger]$. Then we solve the equation

$$\begin{aligned}[\mathbf{1} - \bar{\boldsymbol{Q}}\boldsymbol{S}^\dagger]\vec{c}_\alpha &= \vec{e}_\alpha\\ \vec{s}_\alpha &= \boldsymbol{S}^\dagger\vec{c}_\alpha\end{aligned} \tag{2.23}$$

for $\vec{c}_\alpha$ first using a standard routine for linear equation systems. From the result $\vec{c}_\alpha$, we obtain the screened structure constants $\vec{s}_\alpha$ by multiplication with the screened structure constants. Finally we obtain the screened structure constants as

$$\bar{S}^\dagger_{\gamma,\alpha} = \left(\vec{s}_\alpha\right)_\gamma \tag{2.24}$$

Note that the screened structure constants calculated on finite clusters are no more exactly hermitean.

2.4 Augmentation and Potential parameters

2.4.1 Local orbitals

The local orbitals have the form

$$|\chi_\alpha\rangle = |\phi^K_\alpha\rangle - \sum_{R,L} |\phi^{\bar{J}}_{R,L}\rangle \bar{S}^\dagger_{R,L,R_\alpha,L_\alpha} + \sum_{R',L'} |K^I_{R',L'}\rangle \left[\delta_{R',L',R_\alpha,L_\alpha} - \bar{Q}_{R',L'} \bar{S}^\dagger_{R',L',R_\alpha,L_\alpha}\right] \tag{2.25}$$

wherethe new partial waves $|\phi^K_\alpha\rangle$ and $|\phi^{\bar{J}}_\alpha\rangle$ are superpositions of the valence and scattering partial waves that match differentiably to the head and tail functions $|K_\alpha\rangle$ and $|\bar{J}_\alpha\rangle$.

$$|\phi^K_\alpha\rangle = \overbrace{|\phi_\alpha\rangle \underbrace{\frac{W_\alpha[K,\dot{\bar{\phi}}]}{W_\alpha[\phi,\dot{\bar{\phi}}]}}_{Ktophi} - |\dot{\bar{\phi}}_\alpha\rangle \underbrace{\frac{W_\alpha[K,\phi]}{W_\alpha[\phi,\dot{\bar{\phi}}]}}_{-Ktophidot}}^{\rightarrow |K^\Omega_\alpha\rangle}$$

$$|\phi^{\bar{J}}_{R,L}\rangle = \overbrace{|\dot{\bar{\phi}}_\beta\rangle \underbrace{\left(-\frac{W_\beta[\bar{J},\phi]}{W_\beta[\phi,\dot{\bar{\phi}}]}\right)}_{JBARtophidot}}^{\rightarrow |\bar{J}^\Omega_\beta\rangle} \tag{2.26}$$

Note, that in the factor $JBARTOPHIDOT$ does not depend on the choice of $|\phi\rangle$.

With $W_\alpha[f,g]$ we denote the **Wronskian**

$$W_\alpha[f,g] \stackrel{\text{def}}{=} f_\alpha(\partial_r g_\alpha) - (\partial_r f_\alpha) g_\alpha = \det \begin{bmatrix} f & g \\ \partial_r f & \partial_r g \end{bmatrix} \tag{2.27}$$

which is used to match two functions differentiably to a third via

$$y(x) \to f(x)\frac{W[y,g]}{W[f,g]} + g(x)\frac{W[y,f]}{W[g,f]} \tag{2.28}$$

The matrix elements $\langle \tilde{p}_\gamma | \tilde{\chi}_\alpha \rangle$, which will be needed later, have the form

$$\begin{aligned} \langle \tilde{p}_\gamma | \tilde{\chi}_\alpha \rangle &= \langle \tilde{p}_\gamma | \tilde{\phi}^K_\alpha \rangle - \sum_{R',L'} \langle \tilde{p}_\gamma | \tilde{\phi}^{\bar{J}}_{R',L'} \rangle \bar{S}^\dagger_{R,L,R_\alpha,L_\alpha} \\ &= \langle \tilde{p}_\gamma | \tilde{\phi}^K_\alpha \rangle - \langle \tilde{p}_\gamma | \tilde{\phi}^{\bar{J}}_{R_\gamma,L_\gamma} \rangle \bar{S}^\dagger_{R_\gamma,L_\gamma,R_\alpha,L_\alpha} \end{aligned} \tag{2.29}$$

2.5 Coefficients of the tight-binding orbital

2.5.1 Introduction

In this section, I describe how to determine the wave functions in terms of local orbitals, if the projections $\langle \tilde{p}_\gamma | \tilde{\psi} \rangle$ onto the pseudo wave functions are known.

The basic idea is to find a representation of the wave function in terms of local orbitals $|\chi_\alpha\rangle$

$$|\psi'_n\rangle = \sum_\alpha |\chi_\alpha\rangle q_\alpha \ , \tag{2.30}$$

such that the deviation from the true wave function $|\psi_n\rangle$ is as small as possible.

Ideally, this would amount to minimizing the mean-square deviation of the orbital expansion from the wave function.

$$Q'[\vec{q}] := \Big(\langle\psi_n| - \sum_\alpha q^*_\alpha \langle\chi_\alpha|\Big)\Big(|\psi_n\rangle - \sum_\beta |\chi_\beta\rangle q_\beta\Big)$$

Because evaluating the mean square deviation as integral over all space is time consuming, we limit the integral to the augmentation spheres.

$$\begin{aligned} Q[\vec{q}] &:= \Big(\langle\tilde{\psi}_n| - \sum_\alpha q^*_\alpha \langle\tilde{\chi}_\alpha|\Big)\Big[\sum_{\delta,\gamma} |\tilde{p}_\delta\rangle\langle\phi_\delta|\theta_{\Omega_{R_\delta}}|\phi_\gamma\rangle\langle\tilde{p}_\gamma|\Big]\Big(|\tilde{\psi}_n\rangle - \sum_\beta |\tilde{\chi}_\beta\rangle q_\beta\Big) \\ &= \sum_\gamma \Big[\sum_\delta \Big(\langle\tilde{\psi}_n|\tilde{p}_\delta\rangle - \sum_\alpha q^*_\alpha \langle\tilde{\chi}_\alpha|\tilde{p}_\delta\rangle\Big)\langle\phi_\delta|\theta_{\Omega_{R_\delta}}|\phi_\gamma\rangle\Big]\Big(\langle\tilde{p}_\gamma|\tilde{\psi}_n\rangle - \sum_\beta \langle\tilde{p}_\gamma|\tilde{\chi}_\beta\rangle q_\beta\Big) \end{aligned} \tag{2.31}$$

where $\theta_{\Omega_{R_\delta}}$ is a step function that vanishes outside the augmentation sphere at R_δ.

Minimization yields

$$\frac{\partial Q}{\partial q^*_\alpha} = -\sum_\gamma \Big[\sum_\delta \langle\tilde{\chi}_\alpha|\tilde{p}_\delta\rangle\langle\phi_\delta|\theta_{\Omega_{R_\delta}}|\phi_\gamma\rangle\Big]\Big(\langle\tilde{p}_\gamma|\tilde{\psi}_n\rangle - \sum_\beta \langle\tilde{p}_\gamma|\tilde{\chi}_\beta\rangle q_\beta\Big) \stackrel{!}{=} 0$$

$$\Rightarrow \qquad \sum_\gamma \Big[\sum_\delta \langle\tilde{\chi}_\alpha|\tilde{p}_\delta\rangle\langle\phi_\delta|\theta_{\Omega_{R_\delta}}|\phi_\gamma\rangle\Big]\langle\tilde{p}_\gamma|\tilde{\psi}_n\rangle = \sum_{\gamma,\beta}\Big[\sum_\delta \langle\tilde{\chi}_\alpha|\tilde{p}_\delta\rangle\langle\phi_\delta|\theta_{\Omega_{R_\delta}}|\phi_\gamma\rangle\Big]\langle\tilde{p}_\gamma|\tilde{\chi}_\beta\rangle q_\beta\Big)$$

$$\Rightarrow \qquad q_\beta = \sum_\beta \Big[\sum_{\gamma',\delta'} \langle\tilde{\chi}_\alpha|\tilde{p}_{\delta'}\rangle\langle\phi_{\delta'}|\theta_{\Omega_{R_\delta}}|\phi_{\gamma'}\rangle\langle\tilde{p}_{\gamma'}|\tilde{\chi}_\beta\rangle\Big]^{-1}\Big[\sum_{\gamma\delta}\langle\tilde{\chi}_\alpha|\tilde{p}_\delta\rangle\langle\phi_\delta|\theta_{\Omega_{R_\delta}}|\phi_\gamma\rangle\Big]\langle\tilde{p}_\gamma|\tilde{\psi}_n\rangle \tag{2.32}$$

This allows one to write the wave function in the form

$$|\psi_n\rangle \approx \sum_\alpha |\chi_\alpha\rangle\langle\tilde{\pi}_\alpha|\tilde{\psi}_n\rangle \tag{2.33}$$

with

$$\langle\tilde{\pi}_\alpha| = \sum_\gamma \Big[\sum_{\gamma',\delta'} \langle\tilde{\chi}_\alpha|\tilde{p}_{\delta'}\rangle\langle\phi_{\delta'}|\theta_{\Omega_{R_\delta}}|\phi_{\gamma'}\rangle\langle\tilde{p}_{\gamma'}|\tilde{\chi}_\beta\rangle\Big]^{-1}\Big[\sum_\delta \langle\tilde{\chi}_\alpha|\tilde{p}_\delta\rangle\langle\phi_\delta|\theta_{\Omega_{R_\delta}}|\phi_\gamma\rangle\Big]\langle\tilde{p}_\gamma| \tag{2.34}$$

This expression works also if the number of local orbitals $|\chi_\alpha\rangle$ is smaller than the number of projector functions $\langle p_\gamma|$. Because of the inversion, The multicenter expansion for the projector function is long-ranged so that this expression needs to be evaluated in a Bloch representation.

2.5.2 Transformation between local-orbital and partial-wave projections

In the previous section, I derived in Eq. 2.34 a relation between orbital and partial wave projector functions.

$$\langle\tilde{\pi}_\alpha|\tilde{\psi}_n\rangle = \sum_\beta M_{\alpha,\beta}\langle\tilde{p}_\alpha|\tilde{\psi}_n\rangle \tag{2.35}$$

This operation is performed in `lmto$projtontbo` with `ID='FWRD'`

The derivatives are correspondingly derived as

$$\begin{aligned}
dE &= \sum_{\alpha,\beta} \underbrace{\frac{dE}{d\rho_{\alpha,\beta}}}_{=:h_{\beta,\alpha}} d\rho_{\alpha,\beta} \\
&= \sum_{\alpha,\beta} h_{\beta,\alpha}\Big[\sum_n \langle\pi_\alpha|d\psi_n\rangle f_n\langle\psi_n|\pi_\beta\rangle + \sum_n \langle\pi_\alpha|\psi_n\rangle f_n\langle d\psi_n|\pi_\beta\rangle\Big] \\
&= \sum_n\sum_\alpha f_n \underbrace{\sum_\beta \langle\psi_n|\pi_\beta\rangle h_{\beta,\alpha}}_{HTBC^\dagger_{n,\alpha}}\langle\pi_\alpha|d\psi_n\rangle + \sum_n\sum_\beta \langle d\psi_n|\pi_\beta\rangle \underbrace{\sum_\alpha h_{\beta,\alpha}\langle\pi_\alpha|\psi_n\rangle}_{HTBC_{\beta,n}} f_n \\
&= \sum_n\sum_\gamma f_n \underbrace{\sum_\alpha \underbrace{\sum_\beta \langle\psi_n|\pi_\beta\rangle h_{\beta,\alpha}}_{HTBC^\dagger_{n,\alpha}} M_{\alpha,\gamma}\langle\tilde{p}_\gamma|d\tilde{\psi}_n\rangle}_{HPROJ^\dagger_{n,\gamma}} \\
&+ \sum_n\sum_\gamma \langle d\tilde{\psi}_n|\tilde{p}_\gamma\rangle \underbrace{\sum_\beta M^\dagger_{\gamma,\beta} \underbrace{\sum_\alpha h_{\beta,\alpha}\langle\pi_\alpha|\psi_n\rangle}_{HTBC_{\beta,n}}}_{HPROJ_{\gamma,n}} f_n
\end{aligned} \tag{2.36}$$

Thus, we first define the Hamiltonian ***h*** (HAMIL)

$$\begin{aligned}
\underbrace{h_{\alpha,\beta}}_{HAMIL} &= \frac{dE}{\rho_{\beta,\alpha}} \\
HTBC_{\beta,n} &= \sum_\alpha \underbrace{h_{\beta,\alpha}}_{HAMIL}\underbrace{\langle\tilde{\pi}_\alpha|\tilde{\psi}_n\rangle}_{TBC_{\alpha,n}} \\
HPROJ_{\gamma,n} &= \sum_\beta M^\dagger_{\gamma,\beta}\cdot HTBC_{\beta,n}
\end{aligned} \tag{2.37}$$

This operation is performed in `lmto$projtontbo` with `ID='BACK'`.

2.6 Tailed representation of the natural tight-binding orbitals

The tailed representation replaces the multi-center expansion of the natural tight-binding orbitals by a one-center expansion. The underlying idea the short-ranged tails of the screened orbitals

can be approximatd by exponential tails, that are matched to the one-center expansion of the orbitals at the central site. Thus both the head and the tail functions centered on the central site are extended by a superposition of exponential tails.

2.7 Core-valence exchange

The exchange term between core and valence electrons acts like a fixed, nonlocal potential acting on the electrons, of the form[8]

$$\hat{\tilde{v}}_{x,cv} = \sum_{\alpha,\beta} |\tilde{p}_\alpha\rangle M_{\alpha,\beta} \langle\tilde{p}_\beta| \tag{2.38}$$

The core-valence exchange is furthermore diagonal in the site indices.

$$\begin{aligned}
\langle\chi_\alpha|\hat{v}_{x,cv}|\chi_\beta\rangle &= \sum_{\gamma,\delta} \langle\chi_\alpha|p_\gamma\rangle M_{\gamma,\delta} \langle p_\delta|\chi_\beta\rangle \\
&= \sum_{\gamma,\delta} \langle\tilde{\phi}^K_\alpha|\tilde{p}_\gamma\rangle M_{\gamma,\delta} \langle\tilde{p}_\delta|\tilde{\phi}^K_\beta\rangle \\
&- \sum_{\gamma,\delta,\beta'} \langle\tilde{\phi}^K_\alpha|\tilde{p}_\gamma\rangle M_{\gamma,\delta} \langle\tilde{p}_\delta|\tilde{\phi}^{\bar{J}}_{\beta'}\rangle \bar{S}^\dagger_{\beta',\beta} \\
&- \sum_{\gamma,\delta,\alpha',\alpha} \bar{S}_{\alpha,\alpha'} \langle\tilde{\phi}^{\bar{J}}_{\alpha'}|\tilde{p}_\gamma\rangle M_{\gamma,\delta} \langle\tilde{p}_\delta|\tilde{\phi}^K_\beta\rangle \\
&+ \sum_{\gamma,\delta,\alpha',\alpha} \bar{S}_{\alpha,\alpha'} \langle\tilde{\phi}^{\bar{J}}_{\alpha'}|\tilde{p}_\gamma\rangle M_{\gamma,\delta} \langle\tilde{p}_\delta|\tilde{\phi}^{\bar{J}}_{\beta'}\rangle \bar{S}^\dagger_{\beta',\beta}
\end{aligned} \tag{2.39}$$

Here we used the augmented Hankel and screened Bessel fucntions, respectively their pseudo versions.

As usual we build the expanded density matrix

$$\begin{pmatrix} \boldsymbol{\rho} & -\boldsymbol{\rho}\bar{\boldsymbol{S}}^\dagger \\ -\bar{\boldsymbol{S}}\boldsymbol{\rho} & \bar{\boldsymbol{S}}\boldsymbol{\rho}\bar{\boldsymbol{S}}^\dagger \end{pmatrix} \tag{2.40}$$

The matrix

$$\begin{pmatrix} \langle\tilde{\phi}^K|\tilde{p}\rangle \boldsymbol{M} \langle\tilde{p}|\tilde{\phi}^K\rangle & \langle\tilde{\phi}^K|\tilde{p}\rangle \boldsymbol{M} \langle\tilde{p}|\tilde{\phi}^{\bar{J}}\rangle \\ \langle\tilde{\phi}^{\bar{J}}|\tilde{p}\rangle \boldsymbol{M} \langle\tilde{p}|\tilde{\phi}^K\rangle & \langle\tilde{\phi}^{\bar{J}}|\tilde{p}\rangle \boldsymbol{M} \langle\tilde{p}|\tilde{\phi}^{\bar{J}}\rangle \end{pmatrix} \tag{2.41}$$

is calculated first using `potpar1(isp)%prok` and `potpar1(isp)%projbar`. [9]

[8] Note that this matrix $\boldsymbol{M}$ differs from the one with the same symbol in the previous section.

[9] In the earlier version the contribution from the $\dot{\bar{\phi}}$ has been ignored!!! It has been verified by temporarily switching off the jbar contributiuon to potpar1(isp)%prok and potpar1(isp)%projbar. In this old version only potpar(isp)%ktophi is used to extract the ϕ contribution.

2.8 U-tensor

2.9 Double-counting correction

The double-counting correction is that of Eq. 36 of the paper by Blöchl, Walther, Pruschke[3].

$$E_{xc}^{\hat{W}_R} = \int d^3r \; n_R^\chi(\vec{r})\epsilon_{xc}[n_{\sigma,\sigma'}^\chi(\vec{r})]\frac{n_R^\chi(\vec{r})}{n^\chi(\vec{r})} \tag{2.42}$$

The exchange correlation density is calculated with the correlated orbitals, but there is an additional factor, which cuts of the exchange correlation contribution at large radii, where the density vanishes.

Let us simplify the expression by introducing the symbols $n_R = n_R^\chi(\vec{r})$ and $n_t = n_{\sigma,\sigma'}^\chi(\vec{r})$. With n_R^s and n_t^s we denote the spherical parts of the respective densities.

If the frozen-core density is employed, the contribution of the core must not be included in the double counting term.

The expression above can be written in the following form:

$$\begin{aligned} E_{xc}^{\hat{W}_R} &= \int d^3r \left[n_t(\vec{r})\epsilon_{xc}[n_t(\vec{r})] - n^{core}(\vec{r})\epsilon_{xc}[n^{core}(\vec{r})]\right]\left(\frac{n_R^s(\vec{r})}{n_t^s(\vec{r})}\right)^2 \\ &= \int d^3r \; f_{xc}(\vec{r})\left(\frac{n_R^s(\vec{r})}{n_t^s(\vec{r})}\right)^2 \end{aligned} \tag{2.43}$$

With $f_{xc} := n_t\epsilon_{xc}[n_t] - n^{core}\epsilon_{xc}[n^{core}]$ and $\mu_{xc} := \frac{df_{xc}}{dn_t}$, we obtain

$$\begin{aligned} dE_{xc}^{\hat{W}_R} &= \int d^3r \left(\frac{n_R^s}{n_t^s}\right)^2 \mu_{xc}dn_t + f_{xc}2\left(\frac{n_R^s}{n_t^s}\right)^2\frac{dn_R^s}{n_R^s} - f_{xc}2\left(\frac{n_R^s}{n_t^s}\right)^2\frac{dn_t^s}{n_t^s} \\ &= \int d^3r \left[\left(\frac{n_R^s}{n_t^s}\right)^2\mu_{xc} - 2f_{xc}^s\left(\frac{n_R^s}{n_t^s}\right)^2\frac{1}{n_t^s}\right]dn_t + \left[2f_{xc}^s\left(\frac{n_R^s}{n_t^s}\right)^2\frac{1}{n_R^s}\right]dn_R^s \end{aligned} \tag{2.44}$$

which yields the two potentials

$$\begin{aligned} v_t &\stackrel{\text{def}}{=} \left(\frac{n_R^s}{n_t^s}\right)^2\left[\mu_{xc} - \frac{2f_{xc}^s}{n_t^s}\right] \\ v_R &\stackrel{\text{def}}{=} \left(\frac{n_R^s}{n_t^s}\right)^2\frac{2f_{xc}^s}{n_R^s} \end{aligned} \tag{2.45}$$

For the cutoff function $(n_R^s/n_t^s)^2$ we consider only the spherical contributions of the density and we ignore the spin contributions. This is accounted for in the derivations by only considering the spherical part f_{xc}^s of f_{xc}, while maintaining the non-spherical contributions to μ_{xc}.

The total density n_t contains also the core density. If the core valence Fock term is included, they are part of the correlated electrons and need to be considered in the density n_R.

The double counting correction has the negative sign, because the DFT-expression needs to be subtracted.[10] Its energy and the corresponding contributions to the auxiliary Hamiltonian are

$$\begin{aligned} E_{dc} &= -\int d^3r \left(\frac{n_R^s}{n_t^s}\right)^2 f_{xc}^s \\ d\hat{\tilde{H}}_{dc} &= -|\tilde{\pi}_\alpha\rangle\langle\chi_\alpha|\hat{v}_t|\chi_\beta\rangle\langle\tilde{\pi}_\beta| - |\tilde{p}_\alpha\rangle\langle\phi_\alpha|\hat{v}_R|\phi_\beta\rangle\langle\tilde{p}_\beta| \end{aligned} \tag{2.46}$$

[10] This subtraction is done outside the routine calculating the double counting term.

We start from two density matrices, which are the same at the moment.
see `lmto_simpledc_new`.

Idea

$$E_{xc}^{\hat{W}_R} = \sum_{a,b,c,d} \int d^3r \; \chi_a^*(r)\chi_b(r)\chi_d^*(r)\chi_c(r)\frac{\epsilon_{xc}[n^{\chi}_{\sigma,\sigma'}(\vec{r})]}{n^{\chi}(\vec{r})} \tag{2.47}$$

Chapter 3

Description of Subroutines

3.1 Workflow

```
---initialization----- POTPAR = potential parameters SBAR = screened
 structureconstants <ptilde|chitilde> tailed partial waves overlap
 (Onsite) utensor (Onsite) utensor (offsite) ...  ----cycle-----------
 TBC=<pi-tilde|psi> from PROJ=<ptilde|psitide> DENMAT density matrix
 in local orbitals ...  total energy and derivatives HAMIL hamiltonian
 matrix in tight-binding orbitals ...  HTBC = de/dtbc * 1/f HPROJ =
 de/dproj * 1/f
```

3.2 LMTO$CLUSTERSTRUCTURECONSTANTS

LMTO\$CLUSTERSTRUCTURECONSTANTS calculates the screened structure constants SBAR ($\bar{S}$) for a cluster of NAT atomic sites RPOS, of which the first site is called the central site of the cluster. The number of angular momenta on each site is defined by LX. The screening is defined by the vector QBAR ($\bar{Q}$). K2 ($\vec{k}^2 = -\kappa^2$) is the squared wave vector. (For envelope functions that fall off exponentially, this parameter is negative.)

```
SUBROUTINE LMTO$CLUSTERSTRUCTURECONSTANTS(K2,NAT,RPOS,LX,QBAR,NORB,N,SBAR)
REAL(8)   ,INTENT(IN) :: K2
INTEGER(4),INTENT(IN) :: NAT         ! NUMBER OF ATOMS ON THE CLUSTER
REAL(8)   ,INTENT(IN) :: RPOS(3,NAT) ! ATOMIC POSITIONS ON THE CLUSTER
INTEGER(4),INTENT(IN) :: LX(NAT)     ! X(ANGULAR MOMENTUM ON EACH CLUSTER)
INTEGER(4),INTENT(IN) :: N
REAL(8)   ,INTENT(IN) :: QBAR(N)
INTEGER(4),INTENT(IN) :: NORB
REAL(8)   ,INTENT(INOUT):: SBAR(NORB,N)
```

First, the bare structure constants are evaluates on the cluster using LMTO\$STRUCTURECONSTANTS and then the structure constants are screened using LMTO\$SCREEN.

3.2.1 LMTO$STRUCTURECONSTANTS

`LMTO\$STRUCTURECONSTANTS` calculates the bare structure constants for a pair of sites. The first site is at the origin, where the Hankel function is centered, and the second site at $\vec{R}$ specified by `R21`, is the center of the expansion into solid Bessel functions.

```
subroutine lmto$structureconstants(r21,K2,L1x,L2x,S)
REAL(8)   ,INTENT(IN) :: R21(3) ! EXPANSION CENTER
INTEGER(4),INTENT(IN) :: L1X
INTEGER(4),INTENT(IN) :: L2X
REAL(8)   ,INTENT(IN) :: K2 ! 2ME/HBAR**2
REAL(8)   ,INTENT(OUT):: S((L1X+1)**2,(L2X+1)**2)
```

The bare structure constants are evaluated in `LMTO$STRUCTURECONSTANTS` as

$$S_{RL,R'L'} \overset{\text{Eq. } 2.7}{=} (-1)^{\ell'+1} 4\pi \sum_{L''} C_{L,L',L''} H_{L''}(\vec{R}' - \vec{R}) \begin{cases} (-ik)^{\ell+\ell'-\ell''} & \text{for } k^2 > 0 \\ \delta_{\ell+\ell'-\ell''} & \text{for } k^2 = 0 \\ \kappa^{\ell+\ell'-\ell''} & \text{for } k^2 = -\kappa^2 < 0 \end{cases} \tag{3.1}$$

where $H_L(k^2, \vec{R})$ is the solid Hankel function calculated in `LMTO$SOLIDHANKEL`. The solid Hankel function is the solution of the Helmholtz equation, Eq. 2.3.[1]

More information on the solid Hankel function can be found in appendix A.

Remark: Because the Gaunt coefficients vanish for odd $\ell + \ell' - \ell''$, the structure constants are real even for $k^2 > 0$.

3.2.2 LMTO$SCREEN

I describe here what has been implemented as "version 3".

`LMTO$SCREEN` takes the bare structure constants $S_{RL,R'L'}$ connecting all orbitals on a specific cluster with each other and the screening constants $\bar{Q}$ for all orbitals on the cluster. It returns the screened structure constants connecting the orbitals on the central (first) site (1st index) with all orbitals (2nd index).

The structure constants are defined so that

$$\langle K_{RL}| = -\sum_{L'} S_{RL,R'L'} \langle J_{R'L'}| \qquad \text{for } R' \neq R \tag{3.2}$$

First we evaluate

$$\boldsymbol{A} = \mathbf{1} - \bar{\boldsymbol{Q}}\boldsymbol{S}^{\dagger} \tag{3.3}$$

and the vectors $\vec{e}_\alpha$ defined by $(\vec{e}_\alpha)_\beta = \delta_{\beta,\alpha}$. Note that the number of vectors corresponds to the number of orbitals on the central site only. Therefore, these vectors do not build up a complete unit matrix.

[1] The factors and signs of the inhomogeneity need to be confirmed. The equation has been taken from the methods book, chapter *"Working with spherical Hankel and Bessel functions.*

Then we solve the equation system

$$\boldsymbol{A}\vec{c}_\alpha \overset{\text{Eq. } 2.23}{=} \vec{e}_\alpha \tag{3.4}$$

for $\vec{c}_\alpha$ and

$$\vec{s}_\alpha \overset{\text{Eq. } 2.23}{=} \boldsymbol{S}^\dagger \vec{c}_\alpha \tag{3.5}$$

$\left(\vec{s}_\alpha\right)_\beta = \bar{S}^\dagger_{\beta,\alpha}$ contains the transposed screened structure constants. After transposition, $\bar{S}$ is returned.

3.3 Waves object

The data exchange betweeen the waves object and the lmto object is determined by the local-orbital projections $\langle\tilde{\pi}_\alpha|\tilde{\psi}_n\rangle$ specified by the array `THIS%TBC`, which in turn is obtained from the partial-wave projections $\langle\tilde{p}|\tilde{\psi}_n\rangle$.

In `waves$etot`

```
CALL WAVES$TONTBO
-> CALL LMTO$PROJTONTBO('FWRD'...)
..
..
CALL LMTO$ETOT(LMNXX,NDIMD,NAT,DENMAT)
..
..
CALL WAVES$FROMNTBO()
-> CALL LMTO$PROJTONTBO('BACK'...)
..
..
CALL WAVES$FORCE
-> CALL WAVES_FORCE_ADDHTBC
...
CALL WAVES$HPSI
```

$$\begin{aligned}
\vec{F} &= -\sum_\alpha \frac{dE}{d\langle\tilde{p}_\alpha|\psi_n\rangle}\langle\vec{\nabla}_R\tilde{p}_\alpha|\psi_n\rangle + \text{c.c.} \\
&= -\sum_{\alpha,\beta} \frac{dE}{d\langle\tilde{\pi}_\beta|\psi_n\rangle}\frac{d\langle\tilde{\pi}_\beta|\psi_n\rangle}{d\langle\tilde{p}_\alpha|\psi_n\rangle}\langle\vec{\nabla}_R\tilde{p}_\alpha|\psi_n\rangle + \text{c.c.} \\
&= -\sum_{\alpha,\beta} \frac{dE}{d\langle\tilde{\pi}_\beta|\psi_n\rangle}\frac{d\langle\tilde{\pi}_\beta|\psi_n\rangle}{d\langle\tilde{p}_\alpha|\psi_n\rangle}\left[-\langle\vec{\nabla}_r\tilde{p}_\alpha|\psi_n\rangle\right] + \text{c.c.}
\end{aligned}$$

3.4 Offsite matrix elements

The offsite matrix elements are kept in the data type

```
TYPE OFFSITEX_TYPE
 INTEGER(4)         :: NDIS
 INTEGER(4)         :: NF
 REAL(8)   ,POINTER :: OVERLAP(:,:)  ! OVERLAP MATRIX ELEMENTS
 REAL(8)   ,POINTER :: X22(:,:)      !
 REAL(8)   ,POINTER :: X31(:,:)
 REAL(8)   ,POINTER :: BONDU(:,:)
 REAL(8)   ,POINTER :: DIS(:)
 REAL(8)   ,POINTER :: LAMBDA(:)
END TYPE OFFSITEX_TYPE
```

The matrix elements are initialized in `LMTO_initialize`

```
LMTO_TAILEDGAUSSFIT()
   GAUSSIAN_FITGAUSS(GID,NR,W,L,AUX,NE,NPOW2,E,C(:NPOW2,:,LN))
   LMTO_TAILEDGAUSSORBTOYLM()
LMTO_OFFXINT
    LMTO_OFFSITEOVERLAPSETUP  !O(AB)  ->OFFSITEX%OVERLAP
       LMTO_TWOCENTER
    LMTO_OFFSITEX22SETUP      !U(AABB) ->OFFSITEX%X22
       LMTO_TWOCENTER
    LMTO_OFFSITEX31SETUP      !U(AAAB) ->OFFSITEX%X31
       LMTO_TWOCENTER
    LMTO_TAILEDGAUSSOFFSITEU  !U(ABAB) ->OFFSITEX%BONDU
       GAUSSIAN$ZDIRECTION_FOURCENTER(NIJKA,NEA,EA,LMNXA,ORBA &
    LMTO_OFFSITEXCONVERT()
```

The energy contibution is then calculated using offsitex as follows

```
LMTO_OFFSITEXEVAL_NEW(EX)
    LMTO_EXPANDNONLOCAL
    LMTO_EXPANDLOCAL
    SPHERICAL$ROTATEYLM(LMX,ROT,YLMROT)
    LMTO_OFFSITEX22U(ISPA,ISPB, DIS,LMNXTA,LMNXTB,U22,DU22)
       lmto_offsitexvalue
    LMTO_OFFSITEX31U(ISPA,ISPB, DIS,LMNXTA,LMNXTB,U3A1B,DU3A1B)
       lmto_offsitexvalue
    LMTO_OFFSITEX31U(ISPB,ISPA,-DIS,LMNXTB,LMNXTA,U3B1A,DU3B1A)
       lmto_offsitexvalue
    LMTO_OFFSITEXBONDU(ISPA,ISPB,DIS,LMNXTA,LMNXTB,BONDU,DBONDU)
       lmto_offsitexvalue
```

3.5 Matrix elements using Gaussians

`LMTO_TAILEDGAUSSOFFSITEU` uses the gauss decomposition of the tailed orbitals in `potpar%tailed%gaussnlf`. In `tailedgaussfit` the following data structure is prepared.

```
POTPAR%TAILED%GAUSSNLF%NIJK
POTPAR%TAILED%GAUSSNLF%NORB
POTPAR%TAILED%GAUSSNLF%NPOW
POTPAR%TAILED%GAUSSNLF%NE
POTPAR%TAILED%GAUSSNLF%E
POTPAR%TAILED%GAUSSNLF%C
```

3.6 Matrix elements on an adaptive grid

```
lmto_twocenter

MODULE LMTO_TWOCENTER_MODULE
LMTO_TWOCENTER
    ADAPT$EVALUATE
       ADAPTINI
       ADAPT_BASICRULE
           ADAPT_INTEGRAND
             LMTO_TWOCENTER_MYFUNC
```

3.7 Routines for reporting

```
LMTO$REPORT(NFIL)
..
LMTO$REPORTOVERLAP(NFIL)
LMTO$REPORTSBAR(NFIL)
LMTO$REPORTDENMAT(NFIL)
LMTO$REPORTHAMIL(NFIL)
LMTO$REPORTPERIODICMAT(NFIL,NAME,NNS,SBAR)
...
LMTO$WRITEPHI(FILE,GID,NR,NPHI,PHI)
```

3.8 Routines for plotting orbitals

There are a three routines that calculate the orbitals either in a spherical-harmonics expansion on radial grids or directly on an array of real-space points.

```
LMTO_TAILEDORBLM(IAT,IORB,NR,LMX,ORB)
LMTO_TAILED_NTBOOFR(IAT,iORB,NP,P,chi)
  LMTO_TAILEDORBLM(IAT,IORB,NR,LMX,ORB)
LMTO_NTBOOFR(IAT,iORB,NP,P,chi)

LMTO_PLOTTAILED()  [OK]
    LMTO_TAILEDORBLM(IAT,IORB,NR,LMX,ORB)
LMTO_GRIDPLOT(type,iat)  [ok]
    LMTO_GRIDORB_CUBEGRID(R0(:,IAT0),RANGE,N1,N2,N3,ORIGIN,TVEC,P)
```

```
    LMTO_GRIDORB_STARGRID(R0(:,IAT0),RANGE,NDIR,DIR,NRAD,X1D,P)
    LMTO_TAILED_NTBOOFR(TYPE,IAT,iORB,NP,P,chi)
        LMTO_TAILEDORBLM(IAT,IORB,NR,LMX,ORB)
        LMTO_NTBOOFR(IAT,iORB,NP,P,chi)
    LMTO_WRITECUBEFILE
..
LMTO_GRIDPLOT_UNTAILED(IAT0)
    LMTO_GRIDORB_CUBEGRID(R0(:,IAT0),RANGE,N1,N2,N3,ORIGIN,TVEC,P)
    LMTO_GRIDORB_STARGRID(R0(:,IAT0),RANGE,NDIR,DIR,NRAD,X1D,P)
    LMTO_GRIDENVELOPE(RBAS,NAT,R0,IAT0,LMX,NP,P,ENV,ENV1)
    LMTO_GRIDAUGMENT(RBAS,NAT,R0,IAT0,LMX,NP,P,ORB1,ENV1)
    LMTO_GRIDGAUSS(RBAS,NAT,R0,IAT0,LMX,NP,P,ORBG)
    LMTO_WRITECUBEFILE(NFIL,NATCLUSTER,ZCLUSTER,RCLUSTER &
LMTO_PLOTLOCORB(IAT0)
    LMTO_GRIDENVELOPE(RBAS,NAT,R0,IAT0,LM1X,NP,P,ENV,ENV1)
    LMTO_GRIDAUGMENT(RBAS,NAT,R0,IAT0,LM1X,NP,P,ORB1,ENV1)
    LMTO_GRIDGAUSS(RBAS,NAT,R0,IAT0,LM1X,NP,P,ORBG)
    LMTO_WRITECUBEFILE
LMTO_PLOTNTBO(TYPE,IATORB,LMNORB)
    LMTO_GRIDORB_CUBEGRID(CENTER,RADIUS,N1,N2,N3,ORIGIN,TVEC,P)
    LMTO_GRIDORB_STARGRID(CENTER,RADIUS,NDIR,DIR,NR,X1D,P)
    LMTO_TAILED_NTBOOFR(TYPE,IATORB,LMNORB,NP,P,ORB)
    LMTO_NTBOOFR(TYPE,IATORB,LMNORB,NP,P,ORB)
..
LMTO$PLOTWAVE(NFIL,IDIM0,IB0,IKPT0,ISPIN0,NR1,NR2,NR3)
    LMTO$PLOTWAVE_TAILED(NFIL,IDIM0,IB0,IKPT0,ISPIN0,NR1,NR2,NR3)
        WRITEWAVEPLOTC(NFIL,TITLE,RBAS,NAT,R0,ZAT,Q,NAME,XK,NR1,NR2,NR3,WAVE)
```

- `LMTO_TAILEDORBLM(IAT,IORB,NR,LMX,ORB)` calculates a specific orbital on radial grids in a spherical harmonics representation.
- `LMTO_PLOTTAILED()` writes the tailed local orbitals in a spherical harmonics expanion to file, so that the componenst can be viewed by xmgrace. Each orbital is written to a file `CHI5_3.DAT` where 5 is the atom index and 3 is the orbital index.
- `LMTO_TAILED_NTBOOFR(IAT,iORB,NP,P,chi)` calculates a specific tailed orbital on a set of real space points.
- `LMTO_GRIDPLOT_TAILED(IAT0)` writes the orbitals for the specified site to file. It supports a 3D representation with cube files, and one-dimensional representation on a star grid.

Multicenter expansion

First the interstitial orbital is determined

$$
\begin{aligned}
|\bar{K}^I_\alpha\rangle &= |\bar{K}^\infty_\alpha\rangle - \Big[|K^\Omega_\alpha\rangle - \sum_\beta |\bar{J}^\Omega_\beta\rangle \bar{S}^\dagger_{\beta,\alpha}\Big] \\
&= \sum_\beta |K^\infty_\beta\rangle \Big(\delta_{\alpha,\beta} + \bar{Q}_\beta \bar{S}^\dagger_{\beta,\alpha}\Big) - \Big[|K^\Omega_\alpha\rangle - \sum_\beta |\bar{J}^\Omega_\beta\rangle \bar{S}^\dagger_{\beta,\alpha}\Big] \\
&= \sum_\beta |K^\infty_\beta\rangle \Big(\delta_{\alpha,\beta} + \bar{Q}_\beta \bar{S}^\dagger_{\beta,\alpha}\Big) - \Big[|K^\Omega_\alpha\rangle - \sum_\beta \Big(|J^\Omega_\beta\rangle - |K^\Omega_\beta\rangle \bar{Q}_\beta\Big) \bar{S}^\dagger_{\beta,\alpha}\Big] \\
&= \sum_\beta \Big(|K^\infty_\beta\rangle - |K^\Omega_\beta\rangle\Big) \Big(\delta_{\alpha,\beta} + \bar{Q}_\beta \bar{S}^\dagger_{\beta,\alpha}\Big) + \sum_\beta |J^\Omega_\beta\rangle \bar{S}^\dagger_{\beta,\alpha}
\end{aligned}
\tag{3.6}
$$

This implies that within the sphere centered at R_β only the expansion into bare bessel functions survive, while outside only the bare Hankel function is considered.

Chapter 4

Benchmarks

4.1 Silicon

The files are in ~/Tree/Projects/SetupTests/Si.

I performed calculation for a silicon crystal. We used a mixing of the lcoal exchange of $\alpha_X = 0.1$. The local basiset included one s-type and one p-type tight-binding function.

The following dependencies have been explored:

- kinetic energy of the Hankel function: $K2 = 0, \ldots, -0.5$

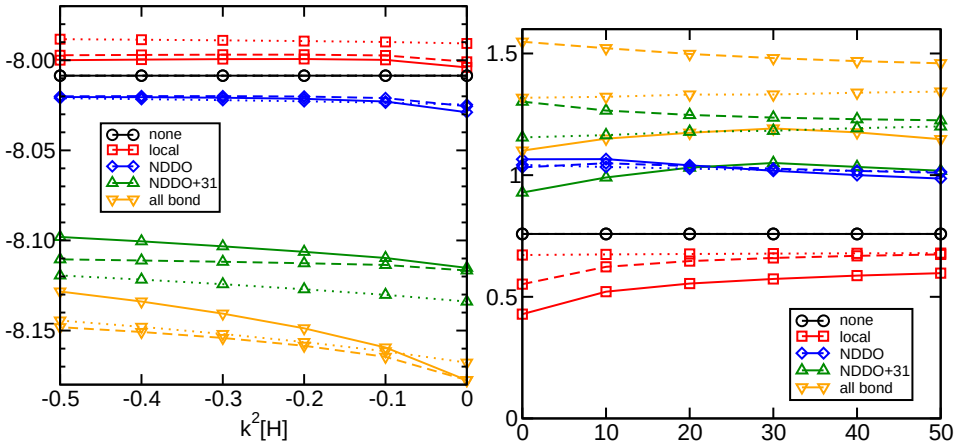

Fig. 4.1: Energy in Hartree and band gap in eV of the silicon crystal as function of the kinetic energy (times -0.01) of the envelope function for the PBE functional (black; none), local Hartree-Fock (red; onsite or local) NDDO-type exchange, i.e density of one site with the density on a bond partner (blue, NDDO), terms with three orbitals on one site and one on the bond partner (green NDDO+31) and the exchange of the bond density with itself (orange, all bond). The full line is the result for one s-type and one p-type orbital. For the dashe4d lines also d-type orbitals are included. The dotted lines are calculated with double orbitals for s,p and single orbitals for d.

- Augmentation radius. The augmentation radius is the radius at which the partial waves

are matched to the envelope function. It is also the radius for the sphere used to derive the projector function onto the local orbitals. The procedure apparently breaks down

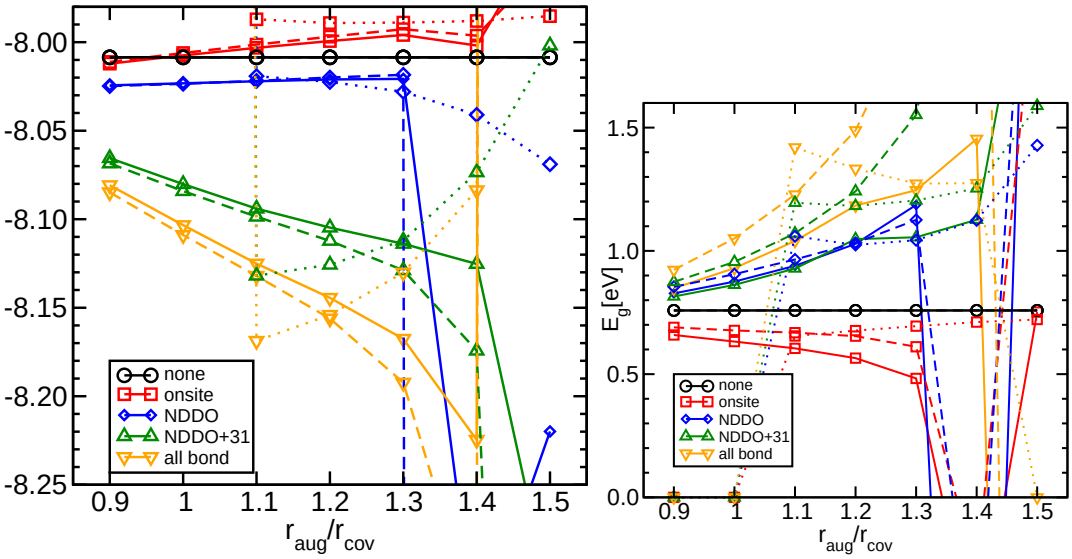

Fig. 4.2: Energy in Hartree and band gap in eV of the silicon crystal as function of the augmentation radius for the PBE functional (black; none), local Hartree-Fock (red; onsite or local) NDDO-type exchange, i.e density of one site with the density on a bond partner (blue, NDDO), terms with three orbitals on one site and one on the bond partner (green NDDO+31) and the exchange of the bond density with itself (orange, all bond). The full line is the result for one s-type and one p-type orbital. For the dashe4d lines also d-type orbitals are included. The dotted lines are calculated with double orbitals for s,p and single orbitals for d.

completely, if the augmentation radius is too large. The dependency becomes stronger, if more non-local terms are included. This may be due to the fact that the double counting term is only included for the local terms.

- tail matching radius

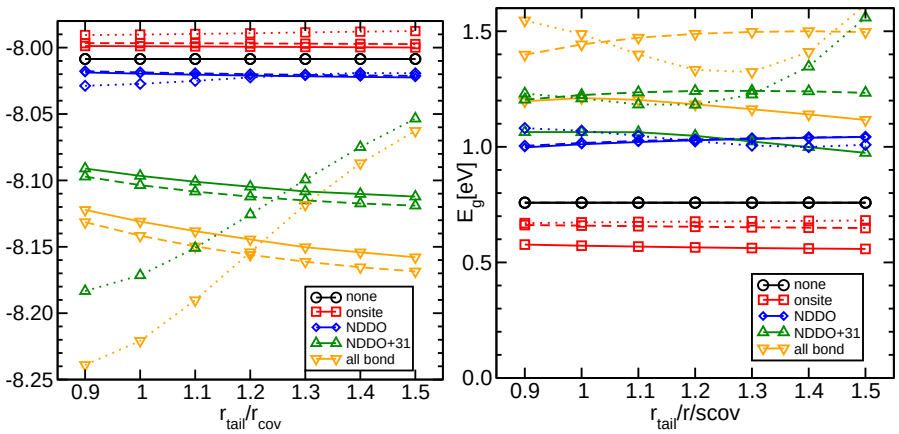

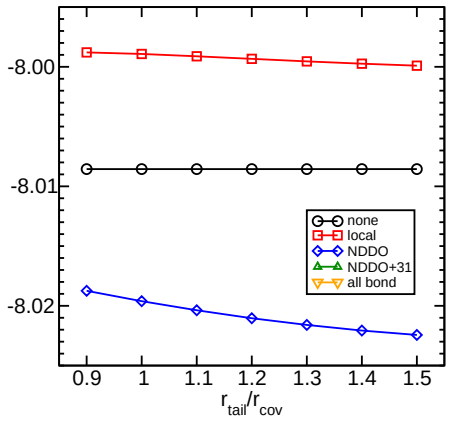

4.1.1 Summary

- The augmentation radius has the largest effects on the results both for the gap and for the total energy. Beyond a certain radius ($> 1.2\ r_{cov}$) the calculation becomes even unstable. For an "overcomplete TB-basisset $2s+2p+1d$ teh calculationb also fails for ($< 1.1\ r_{cov}$).

- It becomes evident that the energy is rather insensitive to the parameters describing the local orbitals for local exchange and the NDDO terms. Additional terms such as "31" and "bondx", which include the bond overlap density $\chi_R(r)\chi_{R'}(r)$ lead to a very strong dependency on the choice of orbitals. Note that 0.05 H≈1.4 eV!

  This may be due to the poor description of the bond density by the exponential tails ofg the tailed orbitals.

  It may also be due to the fact the these terms are not compensated by the double counting term.

- It should be noted that the double counting term is included only for local exchange.

- Choose value of $-0.2 < k^2 < -0.5$ H

- Choose value of $r_{tail} = 1.2 r_{cov}$

Appendix A

Definition of solid Hankel functions

The solid Hankel function has the form

$$H_L(\vec{R}) = Y_L(\vec{R}) \begin{cases} n_\ell(\sqrt{k^2}\cdot|\vec{R}|)\cdot\sqrt{k^2}^{\ell+1} & \text{for } k^2>0 \text{ (Abramovitz 10.1.26)} \\ m_\ell(\sqrt{-k^2}\cdot|\vec{R}|)\cdot\sqrt{\frac{2}{\pi}}\sqrt{-k^2}^{\ell+1} & \text{for } k^2<0 \text{ (Abramovitz 10.2.4)} \\ (2\ell-1)!!|\vec{R}|^{-\ell-1} & \text{for } k^2=0 \text{ (Abramovitz 10.2.5)} \end{cases} \tag{A.1}$$

The solid Hankel function is defined such that the boundary conditions at the origin are independent of k^2.

- the function

$$n_\ell(r) = r^\ell\Big(-\frac{1}{r}\partial_r\Big)^\ell\frac{1}{r}\cos(r) \tag{A.2}$$

  is the spherical Neumann function (see Eq. 8.175 of Cohen Tannoudhi Band 2), which is also called the spherical Bessel function of the second kind. Abramowitz defines $n_\ell(r) = -y_\ell(r)$ (compare Abramowitz Eq. 10.1.26)

  The spherical Neumann function obeys the radial Helmholtz equation (Abramowitz Eq. 10.1.1) for positive kinetic energy

$$\begin{aligned} & r^2\partial_r^2 n_\ell + 2r\partial_r n_\ell + \Big(r^2-\ell(\ell+1)\Big)n_\ell = 0 \\ \Rightarrow\quad & \Big[-\frac{1}{r}\partial_r r + \frac{\ell(\ell+1)}{r^2}\Big]n_\ell(r) = +n_\ell(r) \end{aligned} \tag{A.3}$$

  Note that the subroutine SPFUNCTION$NEUMANN returns the Neumann function with the opposite sign, namely what Abramowitz defines as Bessel function of the second kind. The minus sign is added in the calling routine.

- The function

$$m_\ell(r) = r^\ell\Big(-\frac{1}{r}\partial_r\Big)^\ell\frac{1}{r}\mathrm{e}^{-r} \tag{A.4}$$

  used for $k^2<0$ is obeys the radial Helmholtz equation (Abramowitz Eq. 10.2.1) for negative kinetic energy

$$\begin{aligned} & r^2\partial_r^2 m_\ell + 2r\partial_r m_\ell - \Big(r^2+\ell(\ell+1)\Big)m_\ell = 0 \\ \Rightarrow\quad & \Big[-\frac{1}{r}\partial_r r + \frac{\ell(\ell+1)}{r^2}\Big]m_\ell(r) = -m_\ell(r) \end{aligned} \tag{A.5}$$

They are solutions for negative energy and therefore they fall off exponentially. The solution $m_\ell(r)$ is proportional to the modified spherical Bessel functions of the third kind as defined by Abramowitz[4] in their Eq. 10.2.4.

$$m_\ell(r) = \frac{2}{\pi}\left[\sqrt{\frac{\pi}{2r}}K_{\ell+1}(r)\right] \tag{A.6}$$

which can be verified by comparing the defining equation Eq. A.4 with equations 10.2.24-25 and the definition Eq. 10.2.4 of Abramowitz.

A.1 Bare structure constants

This section is copied from Methods-book, Section "Working with spherical Hankel and Bessel functions", Peter Blöchl, private communication.

The bare structure constants have been determined first by Segall[5]. He uses the theorem[6] that supposedy goes back to Kasterin (N. Kasterin, Proc. Acad. Sci Amsterdam 6, 460 (1897/98)); see Seegall[5], Eq. B4)

$$h_\ell^{(1)}(\kappa r)Y_{\ell,m}(\vec{r}) = i^{-\ell}\mathcal{Y}_{\ell,m}(\vec{\nabla}_r)h_0^{(1)}(\kappa r) \tag{A.7}$$

where $h_\ell^{(1)}(x)$ i the spherical Hankel function of the first kind (see Eq. A.13 below) and where (Eq. B5 of Segall[5])

$$\mathcal{Y}_{\ell,m}(\vec{\nabla}) = \sqrt{\frac{2\ell+1}{4\pi}\frac{(\ell-m)!}{(\ell+m)!}}\left(\frac{1}{ik}\right)^{|m|}\left(\partial_x \pm i\partial_y\right)\mathcal{P}_\ell^{|m|}\left(\frac{1}{ik}\partial_z\right) \tag{A.8}$$

where the positive sign applies for nonzero m and the negative sign for negative m. Furthermore (see Segall[5] Eq. B5)

$$\mathcal{P}_\ell^{|m|}(z) = \frac{d^{|m|}P_\ell(z)}{dz^{|m|}}$$

where $P_\ell(z)$ is the conventional Legendre polynomial.

In addition Segall[5] refers in his Eq. B7 to Morse and Feshbach[7] (part II, p. 1574) for

$$h_0^{(1)}(\kappa|\vec{r}-\vec{r'}|) = 4\pi\sum_L\left(h_\ell^{(1)}(\kappa|\vec{r'}|)Y_L(\vec{r'})\right)j_\ell(\kappa|\vec{r}|)Y_L^*(\vec{r}) \tag{A.9}$$

which is valid for $|\vec{r'}| > |\vec{r}|$.

The two equations, Eq. A.7 and Eq. A.9, can be combined into

$$\begin{aligned}
h_\ell^{(1)}(\kappa|\vec{r}|)Y_{\ell,m}(\vec{r}) &\overset{\text{Eq. A.7}}{=} i^{-\ell}\mathcal{Y}_{\ell,m}(\vec{\nabla}_r)h_0^{(1)}(\kappa|\vec{r}|)\\
&= i^{-\ell}\mathcal{Y}_{\ell,m}(\vec{\nabla}_r)h_0^{(1)}(\kappa|(\vec{r}-\vec{R})+\vec{R}|)\\
&\overset{\text{Eq. A.9}}{=} i^{-\ell}\mathcal{Y}_{\ell,m}(\vec{\nabla}_r)\left[4\pi\sum_{L'}\left(h_{\ell'}^{(1)}(\kappa|\vec{R}|)Y_{L'}(-\vec{R})\right)j_{\ell'}(\kappa|\vec{r}-\vec{R}|)Y_{L'}^*(\vec{r}-\vec{R})\right]\\
&\overset{\text{Eq. A.11}}{=} 4\pi\sum_{L'}\left(i^{-\ell}\mathcal{Y}_{\ell,m}(\vec{\nabla}_R)h_{\ell'}^{(1)}(\kappa|\vec{R}|)Y_{L'}(-\vec{R})\right)j_{\ell'}(\kappa|\vec{r}-\vec{R}|)Y_{L'}^*(\vec{r}-\vec{R})
\end{aligned}$$

Here we used that

$$\vec{\nabla}_r\big[f(\vec{R})g(\vec{r}-\vec{R})\big] = f(\vec{R})\vec{\nabla}_r g(\vec{r}-\vec{R}) = -f(\vec{R})\vec{\nabla}_R g(\vec{r}-\vec{R}) \tag{A.10}$$

$$= -\underbrace{\vec{\nabla}_R \overbrace{\big[f(\vec{R})g(\vec{r}-\vec{R})\big]}^{h(\vec{r})}}_{=0} + \Big[\vec{\nabla}_R f(\vec{R})\Big] g(\vec{r}-\vec{R})\big] \tag{A.11}$$

We summarize the final result

CONDITION FOR STRUCTURE CONSTANTS (POSITIVE ENERGIES)

$$h_\ell^{(1)}(\kappa|\vec{r}|)Y_{\ell,m}(\vec{r}) = 4\pi\sum_{L'}\left(i^{-\ell}\mathcal{Y}_{\ell,m}(\vec{\nabla}_R)h_{\ell'}^{(1)}(\kappa|\vec{R}|)Y_{L'}(-\vec{R})\right) j_{\ell'}(\kappa|\vec{r}-\vec{R}|)Y_{L'}^*(\vec{r}-\vec{R}) \tag{A.12}$$

where $h^{(1)}(x)$ is the spherical Hankel function of the first kind defined in Abramowitz and Stegun (AS)[**?**]

$$h_\ell^{(1)}(x) \overset{AS10.1.1}{=} j_\ell(x) + iy_\ell(x) \overset{AS10.1.26}{=} x^\ell\left(-\frac{1}{x}\partial_x\right)^\ell \frac{\sin(x) - i\cos(x)}{x} \tag{A.13}$$

Expression for the structure constants

By comparing our notation to that of Daniel Grieger and using his expression for the Structure constants, we arrive at the following expression for the structure constants in our notation.

There was a misunderstanding with the sign of the structure constants. Here I follow the signconvention $K = -\sum JS$, which is opposite to the one I and Daniel had earlier.

$$S_{R',L',R,L} = -4\pi\sum_{L''} H^B_{L''}(\vec{R}'-\vec{R})C_{L,L'',L}\begin{Bmatrix}(-1)^{\ell'}(-ik)^{\ell+\ell'-\ell''}\\(-1)^{\ell'}\delta_{\ell+\ell',\ell''}\\(-1)^{\ell'}\kappa^{\ell+\ell'-\ell''}\end{Bmatrix} \tag{A.14}$$

A.2 Consistency checks

We consider the case with $\kappa = 0$, for which the solid Bessel and Hankel functions are

$$K^\infty_{\vec{0},L}(\vec{r}) = (2\ell-1)!!\frac{1}{|\vec{r}|^{\ell+1}}Y_L(\vec{r}) \tag{A.15}$$

$$J_{\vec{0},L}(\vec{r}) = \frac{1}{(2\ell+1)!!}|\vec{r}|^\ell Y_L(\vec{r}) \tag{A.16}$$

The explicit form of the first few is

$$K^{\infty}_{\vec{0},s}(\vec{r}) = \frac{1}{\sqrt{4\pi}}\frac{1}{|\vec{r}|} \tag{A.17}$$

$$K^{\infty}_{\vec{0},p_x}(\vec{r}) = \sqrt{\frac{3}{4\pi}}\frac{x}{|\vec{r}|^3} \tag{A.18}$$

$$J_{\vec{0},s}(\vec{r}) = \frac{1}{\sqrt{4\pi}} \tag{A.19}$$

$$J_{\vec{0},p_x}(\vec{r}) = \frac{1}{3}\sqrt{\frac{3}{4\pi}}x \tag{A.20}$$

Now we extract the structure constants from the off-site expansion

$$\begin{aligned} K^{\infty}_{\vec{0},s}(\vec{r}) = &-S_{\vec{0},s;\vec{R},s}J_s(\vec{r}-\vec{R}) \\ &-S_{\vec{0},s;\vec{R},p_x}J_{p_x}(\vec{r}-\vec{R}) - S_{\vec{0},s;\vec{R},p_y}J_{p_y}(\vec{r}-\vec{R}) - S_{\vec{0},s;\vec{R},p_z}J_{p_z}(\vec{r}-\vec{R}) \end{aligned} \tag{A.21}$$

which allows us to evaluate the structure constants directly calculating value and derivatives at the second center and by exploiting selection rules[1]

$$K^{\infty}_{\vec{0},s}(\vec{R}) = \frac{1}{\sqrt{4\pi}}\frac{1}{|\vec{R}|} = -\underbrace{\left(-\frac{1}{|\vec{R}|}\right)}_{S_{\vec{0},s,\vec{R},s}}\underbrace{\frac{1}{\sqrt{4\pi}}}_{J_{\vec{R},s}(\vec{R})} \tag{A.22}$$

$$\partial_x|_{\vec{R}}\, K^{\infty}_{\vec{0},s} = -\frac{1}{\sqrt{4\pi}}\frac{X}{|\vec{R}|^3} = -\underbrace{\sqrt{3}\frac{X}{|\vec{R}|^3}}_{S_{\vec{0},s;\vec{R},p_x}}\underbrace{\frac{1}{3}\sqrt{\frac{3}{4\pi}}}_{\partial_x J_{\vec{R},p_x}(\vec{R})} \tag{A.23}$$

$$K_{\vec{0},p_x}(\vec{R}) = \sqrt{\frac{3}{4\pi}}\frac{X}{|\vec{R}|^3} = -\underbrace{\left(-\sqrt{3}\frac{X}{|\vec{R}|^3}\right)}_{S_{\vec{0},p_x;\vec{R},s}}\underbrace{\frac{1}{\sqrt{4\pi}}}_{J_{\vec{R},s}(\vec{R})}$$

$$\partial_x|_{\vec{R}}\, K^{\infty}_{\vec{0},p_x} = \sqrt{\frac{3}{4\pi}}\left(\frac{1}{|\vec{R}|^3} - 3\frac{X^2}{|\vec{R}|^5}\right) = -\underbrace{3\frac{3X^2-\vec{R}^2}{|\vec{R}|^2}}_{S_{\vec{0},p_x,\vec{R},p_x}}\underbrace{\frac{1}{3}\sqrt{\frac{3}{4\pi}}|\vec{R}|^{-3}}_{\partial_x|_{\vec{R}}J_{\vec{R},p_x}} \tag{A.24}$$

Thus, the matrix of structure constants in the (s,p_x) subspace is

$$\boldsymbol{S}_{\vec{0},\vec{R}} = \begin{pmatrix} -|\vec{R}|^{-1} & \sqrt{3}X/|\vec{R}|^3 \\ -\sqrt{3}X/|\vec{R}|^3 & 3[3X^2/R^2-1] \end{pmatrix} \tag{A.25}$$

We compare this result now for the one obtained from the direct formula for $\kappa = 0$. These structure constants have the form

$$S_{RL,R'L'} = (-1)^{\ell'+1}4\pi\sum_{L''}C_{L,L',L''}H_{L''}(\vec{R}'-\vec{R})\delta^{\ell+\ell'-\ell''} \tag{A.26}$$

[1] Only an s-function has a finite value at the origin, only a p-function has a finite first derivative at the center, etc.

The structure constants obtained from this equation are

$$
\begin{aligned}
S_{\vec{0},s;\vec{R},s} &= (-1)4\pi \underbrace{\frac{1}{\sqrt{4\pi}}}_{C_{sss}} \cdot \underbrace{\frac{1}{\sqrt{4\pi}} \frac{1}{|\vec{R}|}}_{H_s(\vec{R})} = -\frac{1}{|\vec{R}|} \\
S_{\vec{0},s;\vec{R},p_x} &= 4\pi \underbrace{\frac{1}{\sqrt{4\pi}}}_{C_{p_x,s,p_x}} \underbrace{\sqrt{\frac{3}{4\pi}} \frac{X}{|\vec{R}|^3}}_{H_{p_x}(\vec{R})} = \sqrt{3}\frac{X}{|\vec{R}|^3} \\
S_{\vec{0},p_x;\vec{R},s} &= (-1)4\pi \underbrace{\frac{1}{\sqrt{4\pi}}}_{C_{p_x,s,s}} \sqrt{\frac{3}{4\pi}} \frac{X}{|\vec{R}|^3} = -\sqrt{3}\frac{X}{|\vec{R}|^3} \\
S_{\vec{0},p_x;\vec{R},p_x} &= 4\pi \underbrace{\frac{1}{\sqrt{5\pi}}}_{C_{p_x,p_x,d_{3x^2-r^2}}} \underbrace{\overbrace{\sqrt{\frac{5}{16\pi}} \frac{3X^2-R^2}{|\vec{R}|^2}}^{Y_{3x^2-r^2}} \frac{3}{|\vec{R}|^3}}_{H_{3x^2-r^2}(\vec{R})} = 3\frac{3X^2-R^2}{|R^5|}
\end{aligned}
\tag{A.27}
$$

For Gaunt coefficients see footnote.[2]

[2]

$$
\begin{aligned}
Y_{p_x}Y_{p_x} = \frac{3}{4\pi}\frac{x^2}{r^2} = \frac{1}{4\pi}\frac{x^2}{r^2} + \frac{1}{4\pi}\frac{3x^2-r^2}{r^2} = \frac{1}{\sqrt{4\pi}}Y_s + \frac{1}{4\pi}\sqrt{\frac{16\pi}{5}}Y_{3x^2-r^2} = \frac{1}{\sqrt{4\pi}}Y_s + \sqrt{\frac{1}{5\pi}}Y_{3x^2-r^2} \\
\Rightarrow C_{p_x,p_x,s} = \frac{1}{\sqrt{4\pi}} \qquad \text{and} \qquad C_{p_x,p_x,d_{3x^2-r^2}} = \frac{1}{\sqrt{5\pi}}
\end{aligned}
\tag{A.28}
$$

Appendix B

Bloch theorem revisited

The Bloch states are eigenstates of the discrete lattice translation

$$\hat{S}(\vec{t}) = \int d^3r \; |\vec{r}+\vec{t}\rangle\langle\vec{r}| \tag{B.1}$$

for the discrete lattice vectors $\vec{t}$. The eigenvalue equation has the form

$$\hat{S}(\vec{t})|\psi_{\vec{k}}\rangle = |\psi_{\vec{k}}\rangle e^{i\vec{k}\vec{r}} \tag{B.2}$$

This eigenvalue equation can be recast into the form

$$\langle\vec{r}-\vec{t}|\psi_{\vec{k}}\rangle = \langle\vec{r}|\psi_{\vec{k}}\rangle e^{i\vec{k}\vec{t}} \tag{B.3}$$

This implies that the states can be written as product of a periodic function and a phase factor

$$\langle\vec{r}|\psi_{\vec{k}}\rangle = u_{\vec{k}}(\vec{r})e^{i\vec{k}\vec{r}} \tag{B.4}$$

with

$$u_{\vec{k}}(\vec{r}) = u_{\vec{k}}(\vec{r}+\vec{t}) \tag{B.5}$$

Bloch theorem in a local orbital basis

With $q_\alpha \stackrel{\text{def}}{=} \langle\pi_\alpha|\psi\rangle$, we obtain

$$\begin{aligned}
\hat{S}(\vec{t})\sum_\alpha |\chi_\alpha\rangle q_{\alpha,n} &= \sum_\alpha |\chi_\alpha\rangle q_{\alpha,n} e^{i\vec{k}_n\vec{t}} \\
\int d^3r \; |\vec{r}+\vec{t}\rangle\langle\vec{r}|\sum_\alpha |\chi_\alpha\rangle q_{\alpha,n} &= \int d^3r \; |\vec{r}\rangle\langle\vec{r}|\sum_\alpha |\chi_\alpha\rangle q_{\alpha,n} e^{i\vec{k}_n\vec{t}} \\
\sum_\alpha \langle\vec{r}-\vec{t}|\chi_\alpha\rangle q_{\alpha,n} &= \sum_\alpha \langle\vec{r}|\chi_\alpha\rangle q_{\alpha,n} e^{i\vec{k}_n\vec{t}} \\
\sum_\alpha \langle\vec{r}|\chi_{\alpha+\vec{t}}\rangle q_{\alpha,n} &= \sum_\alpha \langle\vec{r}|\chi_\alpha\rangle q_{\alpha,n} e^{i\vec{k}_n\vec{t}} \\
\sum_{\alpha'} \langle\vec{r}|\chi_{\alpha'}\rangle q_{\alpha'-\vec{t},n} &= \sum_\alpha \langle\vec{r}|\chi_\alpha\rangle q_{\alpha,n} e^{i\vec{k}_n\vec{t}} \\
q_{\alpha+\vec{t},n} &= q_{\alpha,n} e^{-i\vec{k}_n\vec{t}}
\end{aligned} \tag{B.6}$$

Density matrix

$$\rho_{\alpha,\beta+\vec{t}} = \sum_n \langle \pi_\alpha | \psi_n \rangle f_n \langle \psi_n | \pi_\beta \rangle \mathrm{e}^{+i\vec{k}_n\vec{t}} \tag{B.7}$$

Appendix C

Offsite matrix elements using Gaussian integrals

In LMTO_INITIALIZE there are non-functional calls for doing the integrations in a representation of Gauss orbitals. The routines are no more present, except for

- LMTO_TAILEDPRODUCTS. They have been removed in 7501a0g from Feb.2, 2013 (svn revision 1116 from Nov. 20, 2011). LMTO_TAILEDPRODUCTS has been removed after 9803b02 on from Mar. 1, 2014.
- LMTO_EXPANDPRODS

The routines related to Gaussians have been moved into the file paw_lmto_stuffwithgaussians.f90

```
!!$      CALL LMTO_TAILEDPRODUCTS()
              gaussian_fitgauss
!!$      CALL LMTO_GAUSSFITKPRIME()
!!$      CALL LMTO_GAUSSFITKAUGMENT()
!!$      CALL LMTO_GAUSSFITKJTAILS()
!!$      CALL LMTO_ONSITEOVERLAP()
```

Appendix D

Changelog, Bugfixes

- the core-valence exchange contribution differs from the old version, because it also includes the projection on the phidot functions.
- there has been a bug in `lmto$screen`, which has been fixed with version 3. It may be better to rewrite all structure constants routines with teh transposed structure constants.
- in `lmto$makestructureconstants`, the structure constants have not been calculated because the parallelzation was wrong. in 13403f6.

```
-       IF(MOD(IAT1-1,NTASKS).NE.THISTASK-1) THEN
+       IF(MOD(IAT1-1,NTASKS).eq.THISTASK-1) THEN
```

Bibliography

[1] P. E. Blöchl and C. Först. Node-less atomic wave functions, pauli repulsion and systematic projector augmentation. Arxiv, 1210.5937, 2012. URL http://arxiv.org/abs/1210.5937.

[2] O. Krogh Andersen. Linear methods in band theory. Phys. Rev. B, 12:3060–3083, Oct 1975. doi: 10.1103/PhysRevB.12.3060. URL http://link.aps.org/doi/10.1103/PhysRevB.12.3060.

[3] P. E. Blöchl, C. F. J. Walther, and Th. Pruschke. Method to include explicit correlations into density-functional calculations based on density-matrix functional theory. Phys. Rev. B, 84:205101, 2011. doi: 10.1103/PhysRevB.84.205101. URL http://link.aps.org/doi/10.1103/PhysRevB.84.205101.

[4] M. Abramowitz and I.A. Stegun, editors. Handbook of Mathematical Functions with Formulas, Graphs and Mathematical Tables, volume 55 of Applied Mathematics Series. National Bureau of Standards, 1964.

[5] B. Segall. Calculation of the band structure of "complex" crystals. Phys. Rev., 105:108, 1957.

[6] J. Korringa. On the calculation of the energy of a bloch wave in a metal. Physica, 13:392, 1947.

[7] P. M. Morse and H. Feshbach. Methods of Theoretical Physics. McGraw-Hill, NY, 1953.